R-loop accumulation induced by splicing perturbation triggers PARP1/2 response

A Thesis

SUBMITTED TO THE FACULTY OF THE

UNIVERSITY OF MINNESOTA

BY

Dawei Zong

IN PARTIAL FULFILLMENT OF THE REQUIREMENTS

FOR THE DEGREE OF

MASTER OF SCIENCE

Advisor: Dr. Hai Dang Nguyen

Co-advisors: Dr. Anja K. Bielinsky, Dr. Cheuk Leung

June 2022

Acknowledgements

I would like to appreciate my mentor Dr. Hai Dang Nguyen for all the help provided for in-lab research, thesis writing, thank you for training me in these 2 years.

In addition, I would like to appreciate all members in HDN lab: Maxwell Bannister, Victor Corral, Matthew McMahon, Zhiyan (Silvia) Liu, and Gabriel Phelan (ranked in alphabetical order according to surnames) for all the help provided in lab and all the suggestions provided on this thesis; Dr. Anja K. Belinsky and Dr. Cheuk Leung, for all the work done on reviewing this thesis; Dean of University of Minnesota Pharmacology Department Colin Campbell, for giving me the chance to join the MS Pharmacology program and get educated at U of M.

This research was supported by The National Institutes of Health's National Center for Advancing Translational Sciences, grants KL2TR002492 and UL1TR002494, Evans P. Edward Foundation Young Investigator Award, and American Society of Hematology Scholar Award to H.D.N. The content is solely the responsibility of the authors and does not necessarily represent the official views of the National Institutes of Health's National Center for Advancing Translational Sciences.

Abstract

Mutation in genes encoding for *U2AF1*, *SRSF2*, and *SF3B1* are commonly mutated in myelodysplastic syndromes (MDS) and other hematological malignancies, highlighting a unique genetic vulnerability for targeted therapies. Recent studies showed that perturbing RNA splicing by pharmacological modulators selectively sensitizes RNA splicing mutant cancers *in vitro* and *in vivo* models. However, the use of pharmacological modulators in clinical trials did not show improved efficacy in patients carrying RNA splicing factor mutations, pointing to a need for drug combination strategies. We previously reported that RNA splicing perturbation caused by pharmacological splicing modulators trigger aberrant accumulation of R-loops, a three-stranded nucleic acid structure consisting of an RNA:DNA hybrid and a displaced single-stranded DNA and depend on R-loop response signaling for survival. Based on these findings, we hypothesize that targeting different R-loop response pathways enhances cancer cell killing when combined with RNA splicing modulators. Here, we identified that RNA splicing modulator, pladienolide B (Plad-B) elicited a poly ADP-ribosylation (PARP) response in an R-loop dependent manner. PARP inhibitor, olaparib, induced more DNA damage in cells treated Plad-B, suggesting a new therapeutic drug combination that may enhance cell death. Surprisingly, we found that the PARP response in Plad-B treated cells requires both PARP1 and PARP2 function. This is in stark contrast to their known functions in DNA repair where PARP1 plays the dominant role. Taken together, we propose a two-step model where PARP1 initiates and PARP2 amplifies the ADP-ribosylation signaling to prevent R-loop-associated genomic instability. Importantly, our results highlight a new R-loop regulatory signaling mediated by PARP1/2 and a potential of repurposing FDA-approved PARP inhibitors to treat MDS patients harboring splicing factor mutations either as a monotherapy or in combination with RNA splicing modulators.

Table of Contents

List of Figures ..... **iv**

List of Tables ..... **v**

Introduction **1**

Methods **6**

Results **9**

Discussion **22**

Bibliography **26**

List of Figures

Figure 1: 11

Figure 2: 14

Figure 3: 17

Figure 4: 19

Figure 5: 21

Figure 6: 23

Figure 7: 24

List of Tables

Table 1: 7

Introduction

Myelodysplastic syndrome (MDS) is a heterogeneous, malignant bone marrow failure that occur when hematopoietic stem cells (HSC) cannot differentiate and start to dominate in the bone marrow[1]. In MDS, abnormal malignant HSCs gain a growth advantage over normal HSCs, and the resulting daughter cells overwhelm the bone marrow, so that, unlike other hematopoietic malignancies, clonal cells retain the ability to mature[2]. Malignant cells also slow the tissue's ability to create healthy hematopoietic stem cells when they spread through the marrow[3]. As a result, patients have fewer viable blood cells in circulation. MDS is diagnosed primarily in elderly white people and has slightly higher frequency in men than women[4,5]. Approximately 30% of high-risked MDS patients progresses to develop secondary acute myeloid leukemia (sAML), which is a severe and rapidly progressing type of blood cancer[6,7]. There are two existing standard treatment options: hypomethylating agents (HMAs) and allogeneic hematopoietic cell transplantation (HCT)[8]. HMAs (azacitidine, intravenous decitabine, and oral decitabine) are the standard of care for MDS patients. They have been shown as effective in lower-risk and higher-risk MDS, suggesting a role of early intervention using these agents[9]. However, 50% of patients relapse within 2 years and are associated with poor prognosis and limited therapeutic options[10]. HCT can be effective in curing patients who have failed therapy with HMA[11]. However, the complexity of the disease hinders patients from becoming eligible for transplantation procedure. First, finding matched bone marrow donors for HCT is very challenging. Second, patients are prone to infections due to low defective hematopoiesis or develop co-morbidities during the pre-transplantation process. Third, the disease might progress to a high-proliferative stage where HCT is either no longer a suitable treatment option or may yield low success rate. Moreover, increasing age comes with an increasing prevalence of comorbid conditions and poorer tolerance to high intensity therapy before HCT, which may lower successful HCTs[12,13]. Taken together, there remains a high unmet need for new targeted therapeutic strategies for MDS

patients.

Somatic heterozygous mutations in the spliceosome genes, *U2AF1, SRSF2, SB3F1*, and *ZRSR2*, commonly occur in over 50% patients with hematologic malignancies including MDS and sAML, and are mostly mutually exclusive[14,15]. Although the mechanisms by which splicing factor mutations contribute to the pathogenesis of MDS remain unclear, the occurrence of these mutations early in disease development suggests that these may be driver mutations[16], and these mutations are enriched across a spectrum of clonal myeloid disorders including MDS and sAML[17]. Bone marrow cells from patients or from genetically-engineered mouse models harboring missense mutations at specific amino acids in MDS-associated *U2AF1, SRSF2, SF3B1* mutations have been shown RNA splicing perturbation. In contrast, ZRSR2 has nonsense or frameshift mutations in the coding region, and these alterations are expected to result in loss of function. Expression of MDS-associated spliceosome mutations in cell lines also altered RNA splicing[17–20]. Therefore, these studies suggest that cells expressing spliceosome mutations alter RNA splicing, which may have an important contribution to MDS pathophysiology.

RNA splicing removes introns within newly made precursor messenger RNA (pre-mRNA) transcripts to generate mature messenger RNAs (mRNA). RNA splicing process involves several steps that are catalyzed by the spliceosome, a complex of small nuclear ribonucleoproteins (snRNPs): U1, U2, U4, U5 and U6, and their associated proteins[21]. Introns have 5′ and 3′ splice site (SS) and a branch point sequence (BS). These are characterized by consensus nucleotide sequences, which are recognized by the RNA part of the snRNPs. First, RNA splicing is initiated by the binding of U1 snRNP (U1) to the 5′ SS. U2 snRNP binds to the BS. Subsequently, U1 is replaced by a complex of U4-U5-U6 snRNPs. With the participation of U5, the 3′ SS of the intron is brought into proximity, cut, and joined to the 5′ SS. After U4 snRNP is released, U6 and U2 can bind, producing a lariat. Then, the resulting lariat is released with U2, U5 and U6 bound to it, and the exons are joined. This process is

repeated until all introns in the pre-mRNA of a gene are removed[22,23]. However, somatic mutations in *SF3B1, SRSF2,* and *U2AF1* affecting splicing regulatory sequences can alter pre-mRNA splicing, leading to alternative selection of exon inclusion, exon skipping, intron retention, and 5′ or 3′ splice sites[24]. Many aberrantly spliced transcripts have been associated with spliceosome mutations to date, but only a few events are functionally associated with disease phenotypes[25]. This raises the possibility that splicing-independent mechanisms may contribute to MDS disease and may represent novel modalities for targeted therapies.

We and others previously showed that RNA splicing perturbation by either pharmacological modulators or expression of spliceosome mutants, such as U2AF1^{S34F}, increased the aberrant accumulation of R-loops[26,27]. R-loop is a transcription intermediate resulting from a RNA:DNA hybrid and a displaced strand of single-strand DNA (ssDNA)[26]. Importantly, R-loop accumulation is independent of misplicing events in splicing mutant cells. R-loops have physiology functions. For example, R-loop is responsible for class switch recombination for immunoglobulins[28]. R-loop formation correlated with GC skew at promoter protects the region from the primary de novo DNA methyltransferase in early development[29], and promotes a chromatin architecture that defines the termination region for a substantial subset of mammalian genes[30]. However, the aberrant accumulation and/or distribution of R-loop are also associated with genomic instability. The collisions between R-loops and DNA replication forks can generate DNA double-strand breaks (DSBs), which ultimately drive cells to apoptosis if not properly repaired[31]. Therefore, inhibition of R-loop regulators in cancers with the aberrant R-loop accumulation could lead to more DNA damage accumulation and cell death, representing a potential therapeutic treatment for MDS. There are several mechanisms to downregulate R loop in cells. For example, DNA topoisomerase I (TOP1) suppresses the formation of R-loop through SUMOylation removing the negative supercoils behind RNA polymerases[32]. R-loops could be unwound by RNA:DNA helicases, such as Senataxin (SETX) and

Aquarius (AQR), when they are formed[33,34]. Additionally, replication proteins A (RPA), a ssDNA-binding heterotrimeric complex, senses and coats ssDNA which recruits RNase H1 to remove the RNA moiety within RNA:DNA hybrids to resolve R-loops[31,35,36]. Overexpression of RNase H1 is sufficient to reduce R-loops and R-loop-associated genomic instability[26]. RPA at R-loops also elicits ATR, but not ATM, kinase signaling pathway to respond to aberrant R-loops or genomic instability they induce[27]. Cells expressing spliceosome mutations accumulate R-loops and activate R-loop associated ATR kinase for survival[37]. Using specific ATR inhibitors, ATR inhibition induces more DNA damage in leukemia cells expressing mutant splicing factors, selectively kills cells expressing splicing factor mutations. Therefore, targeting R-loop-associated ATR kinase represents a potential targeted therapy for MDS/AML patients harboring splicing factor mutations. Taken together, these studies highlight that targeting distinct R-loop response pathways beyond ATR provides a new therapeutic opportunity in cancers that harbor SF mutations such as MDS and sAML.

Our unpublished work showed that spliceosome mutant leukemias are preferentially sensitive to inhibitors targeting Poly (ADP-Ribose) Polymerase 1/2 (PARP1/2), such as olaparib, veliparib, talazoparib, niraparib, and rucaparib (*Liu and Sinha, et. al., manuscript in prepration*). PARP1 is a member of Poly (ADP-Ribose) Polymerases (PARPs; also known as ADP-ribosyl transferases) family, which catalyze Mono/Poly-ADP-ribosylation (MAR/PAR). ADP-ribosylation involves the transfer of ADP-ribose residues onto target substrates, in response to DNA damage[38,39]. Among 17 PARP family member, PARP1 is a founding member of this family which conducts more than 90% of total PARylation activity at least in response to DNA damage. PARP2, functions as a backup PARP enzyme in the absence of PARP1 and generates less than 10% of total PARylation in response to DNA damage[40]. Therefore, inhibition of PARP1 is an attractive strategy for the treatment of cancers.

Based on our observation that splicing mutant leukemias induced R-loops and trigger PARP1 response, we asked whether the R-loop-associated PARP1/2 response is a

unifying mechanism caused by general RNA splicing perturbation. In my thesis project, I utilized mRNA splicing modulators such as pladienolide B (Plad-B) and MS023 to evaluate R-loop and ADP-ribosylation status. Plad-B is a naturally occurring macrolide that target the splicing factor SF3b1 complex to induce RNA splicing alterations[41–43]. Additionally, MS023, another mRNA splicing modulator, is a Type I protein arginine methyltransferase (PRMT) inhibitor. The PRMT family members methylate multiple components of the splicing machinery to ensure its functionality. Inhibition of type I PRMTs suppresses symmetric or asymmetric dimethylation of arginine reduces splicing fidelity[44–46]. Thus, inhibiting type I PRMTs may simultaneously affect RNA splicing activity and R-loop accumulation. We identified that RNA splicing modulator, Plad-B elicited ADP-ribosylation response in an R-loop dependent manner. PARP inhibitor, olaparib, induced more DNA damage in cells treated Plad-B, suggesting a new drug combination that may enhance cancer cell killing. Surprisingly, we found that both PARP1 and PARP2 enzymes are important for PARP response in Plad-B treated cells, which is in contrast to their known functions in DNA repair where PARP1 plays the major role. PARP1 loss completely abrogated all ADP-ribosylation induced by hydrogen peroxide and Plad-B or MS023. Interestinlgly, while loss of PARP2, but not PARP1, showed no defect in hydrogen peroxide-induced ADP-ribosylation, loss of PARP2 drastically reduced ADP-ribosylation induced by either Plad-B or MS023. These results suggest that both PARP1 and PARP2 play an important role in suppressing R-loop-associated genomic instability in mRNA splicing modulators treated cells. Taken together, our study established a link between R-loop induced PARP1/2 activation and RNA splicing perturbation. We propose a two-step model where PARP1 initiates and PARP2 amplifies the ADP-ribosylation signaling cascade in response to R-loop accumulation. Importantly, our results also highlight a potential of repurposing FDA-approved PARP inhibitors to treat MDS patients harboring splicing factor mutations either as a monotherapy or in combination with RNA splicing modulators.

Methods

Cell culture. HeLa and HEK293T cells were cultured in Dulbecco's modified Eagle's medium (DMEM) supplemented with 10% Fetal Bovine Serum (FBS), 4 mM L-glutamine, and 1% penicillin/streptomycin. To generate HeLa cells expressing GFP-tagged doxycycline-inducible RNase H1, HeLa cells were infected by Lentivirus containing RNaseH1-GFP and were selected by neomycin. 200ng/ml doxycycline for 24h was used to induce expression of RNaseH1-GFP. HeLa cells expressing GFP-tagged doxycycline-inducible RNase H1 were cultured in DMEM medium supplemented with G418 (600 μg/ml). For the generation of stable *PARP1*^{KO} or *PARP2*^{KO} cell lines, HeLa cells were transfected with 2 ug of PX459-sgPARP1-1 plasmid or PX459-sgPARP2-1 plasmid using Lipofectamine 3000 Transfection Reagent (ThermoFisher Scientific) following manufacturer's instructions for 24 hours. Gibco™ Puromycin Dihydrochloride purchased from Fisher Scientific was used for the selection after 24h transfection. After 2 days, the transfected cells were validated for loss of PARP1 or PARP2 protein expression and Plad-B induced PARylation using western blotting. For PARP1 rescue, *PARP1*^{KO} cells were transfected with 2 ug of pCMV-PARP1-3xFlag-WT, pCMV-PARP1-3xFlag-7xKQ, or pCMV-PARP1-3xFlag-E988K plasmid using Lipofectamine 3000 Transfection Reagent. After 24h transfection, the transfected cells were treated with 24H Plad-B and then were analyzed by assessment of MAR/PAR and PARP1 levels by immunoblot. The HeLa cell line was used as a wild-type control.

Generation of PARP1 mutant plasmids. To generate PARP1 mutations from pCMV-PARP1-3xFlag-WT, two oligonucleotide primers were designed for cloning reaction via PCR (Table 1). The PCR products were generated by using Phusion High-Fidelity DNA Polymerase and verified by agarose gel electrophoresis that our target fragment was amplified. The target fragment was collected from agarose gel for purification using Gel/PCR DNA Fragments Extraction Kit. By using the In-Fusion HD Clong Kit, the purified fragments were fused together and transformed into DH5α Competent

Cells (18265017, Invitrogen). All mutations were validated by Sanger sequencing.

Table 1. Primer sequences used for mutagenesis

Mutagenesis	Forward primer	Reverse primer
pCMV-PARP1-3xFlag-ZnF	5'-ATTCCCCtaAAGTACATTGTCTATGATATTGCTCAGG-3'	5'-TGTACTTtaGGGGAATATACGGTCCTGTTTTTTAAC-3'
pCMV-PARP1-3xFlag-ΔBRCT	5'-GAGAATGAAATTAACTCTTAAAGGAGGAG-3'	5'-GTTAATTTCATTCTCTTTTCAGATTTGGGGAATATACGGTCCTGTTTTTTAAC-3'
pCMV-PARP1-3xFlag-ΔWGR	5'-AAGGGCCAGGTCAAGCTGACAGTAAATCCTGGCACCAAG-3'	5'-CTTGACCTGGCCCTTGCTTTTTTTG-3'
pCMV-PARP1-3xFlag-E988K	5'-ATATAACaAGTACATTGTCTATGATATTGCTCAGG-3'	5'-ATGTACTtGTTATATAGTAGAGAGGTGTCATTCAC-3'

Inhibitors and antibodies. Inhibitors used in this study: pladienolide B (16538, Cayman), MS023 (S8112, SelleckChem), Olaparib (AZD2281, SelleckChem), Veliparib (ABT-888, SelleckChem). Antibodies used in this study: anti-pan-ADP-ribose binding reagent (MABE1016, Millipore), Poly/Mono-ADP Ribose (83732, CST), PARP1 (9532, CST), PARP2 (39044, Active Motif), KU70 (4588, CST), Phospho-RPA32 (S33) (A300-246A, Bethyl), RPA32 (MA1-26418, Invitrogen), RPA70 (A300-241A, Bethyl), GFP (A11122, Invitrogen), Flag (F7425, Sigma), Phospho Histone H2A.X (Ser139) (9718S, CST), Phospho Histone H2A.X (Ser139) (05-636, Millipore),

Ku70 (GTX70271, GeneTex).

Immunoblots. Cells were collected and lysed by lysis buffer (100 mM Tris PH 6.8, 1% Sodium dodecyl sulfate). The lysis of cells was denatured at 100 degrees Celsius for 15 min. Protein concentrations were determined by Pierce™ BCA Protein Assay Kit from Fisher and mixed 1:1 with 2× SDS-PAGE loading buffer (100 mM Tris at pH 6.8, 12% glycerol, 3.5% SDS, 0.2 M DTT). Samples were ran on either 8 or 12% polyacrylamide gels at 100V for 90 min. Proteins were transferred onto PVDF membranes for 1.5 h at 250 mA. The membranes were blocked in 5% blocking buffer (ex. 5g Difco™ Skim Milk in 100ml 1x TBST) for 1h and then incubated with primary antibodies overnight at 4°C. Next day, blots were washed with 1x TBST (20 mM Tris, 150 mM NaCl, 0.05% Tween® 20) and incubated with secondary antibodies on the shaker for 1h. Then, the membranes were incubated in Clarity™ Western ECL Substrate for 5 min and visualized with ChemiDoc™ MP Imaging System from BIO-RAD.

Immunofluorescence. HeLa cells were grown on the coverslips in 6-well plates. For one day treatment, 60k cells/ml were seeded. Cells were fixed with 3% PFA/2% sucrose solution on ice for 15 min and washed with cold 1x PBS. Subsequently, cells were permeabilizated with 1x PBS containing 0.5% Triton and treated in the blocking buffer (10% Difco™ Skim Milk, 3% BSA, 0.05% Tween in 1x PBS) on platform shaker at room temperature for 1h. Cells were incubated with primary antibodies for 2h. After the incubation of primary antibodies, cells were washed with 1x PBST (PBS + 0.05% Tween) and incubated with secondary antibodies for 1h. Then, cells were stained with DAPI (1 ug/mL) after final wash of 1x PBS to visualize nuclei. The images were captured by Leica imaging microscope and analyzed by ImageJ software.

Immunoprecipitation. 18h prior to transfection, 2.5 million HEK293T cells were seeded. Cells were transfected with various Flag-tagged PARP1 plasmids expressing either $PARP1^{WT}$, $PARP1^{ZnF}$, $PARP1^{\Delta WGR}$, $PARP1^{\Delta BRCT}$, or $PARP1^{E988K}$ with calcium

phosphate and harvested after 72h. Cell pellets were lysed in NETN lysis buffer (50mM Tris pH 7.5, 150 mM NaCl, 0.5% NP-40, 1mM PMSF, 5mM NaF, 1mM NaOrVa, 1mM DTT, 1x protease inhibitor). Flag-tagged proteins were immunoprecipitated by using 50uL of Anti-FLAG Magnetic Beads (M8823, Sigma) on the rotor in 4℃ cold room overnight. Beads were washed three times with NETN lysis buffer before using. Subsequently, proteins conjugated with beads were washed three times with NETN lysis buffer containing 150 mM NaCl and once with lysis buffer containing 250 mM NaCl.

Results

Pladienolide B induces RNA splicing perturbation and elicits a PARP response through R-loops.

Our unpublished works have established that leukemias expressing either *SRSF2*^{P95H} or *U2AF1*^{S34F} mutations induce R-loops and PARP1 activation (*Liu, Sinha, et. al., manuscript in preparation*). Next, we asked whether RNA splicing perturbation by mRNA splicing modulators would also induce PARP1 response through R-loops. In order to evaluate PARP activity in HeLa cells, we monitored endogenous Mono- and Poly-(ADP-ribosylated) (MAR/PAR) protein levels as a measure of total PARP activity. Pladienolide B (Plad-B), a mRNA splicing modulator which targets SF3B1, the core component of the U2 small nuclear ribonucleoprotein (U2 snRNP) complex, to induce RNA splicing alterations[41–43]. Plad-B treated HeLa cells increased MAR/PAR levels (Figures 1A and 1B, lanes 2). Treating cells with PARPi, olaparib or veliparib, in the presence or absence of Plad-B suppressed the Plad-B induced MAR/PAR levels (Figures 1A and 1B, lanes 3 and lanes 4). Collectively, these results suggest that Plad-B induces ADP-ribosylation in a PARP dependent manner.

Cells treated with Plad-B has been shown to induce R-loops[26,27]. Next, we asked whether the Plad-B-induced MAR/PAR levels arises from R-loop. To address this question, we generated doxycycline inducible GFP-tagged RNase H1^{D210N} (RNase

H1^{D210N}-GFP) expressing HeLa cells. RNase H1^{D210N} mutation abolishes the catalytic activity of RNase H1 but it retains binding affinity to RNA:DNA hybrids. Therefore, RNase H1^{D210N}-GFP can be applied to fixed cells as a versatile imaging tool as a measure of R-loop levels in cells. We treated GFP-tagged RNase H1^{D210N} expressing HeLa cells with either DMSO or Plad-B in the presence of doxycycline for 24h and measured R-loop levels by immunofluorescence using GFP specific antibody. Plad-B treated HeLa cells exhibited higher chromatin-bound RNase H1^{D210N}-GFP levels compared to DMSO treated HeLa cells (Figure 1C), confirming that Plad-B treatment increased R-loop levels as previously reported[26,27]. To test whether PARP activity is R-loop dependent, we generated HeLa cells that expresses a doxycycline inducible GFP-tagged nuclear RNase H1 (RNase H1-GFP) to resolve R-loops. Overexpression of RNase H1-GFP in Plad-B-treated HeLa cells drastically suppressed MAR/PAR level, suggesting that Plad-B induced ADP-ribosylation is R-loop dependent (Figure 1D). Taken together, these results demonstrate that RNA splicing perturbation by mRNA splicing modulator, Plad-B triggers R-loop accumulation and PARP activation.

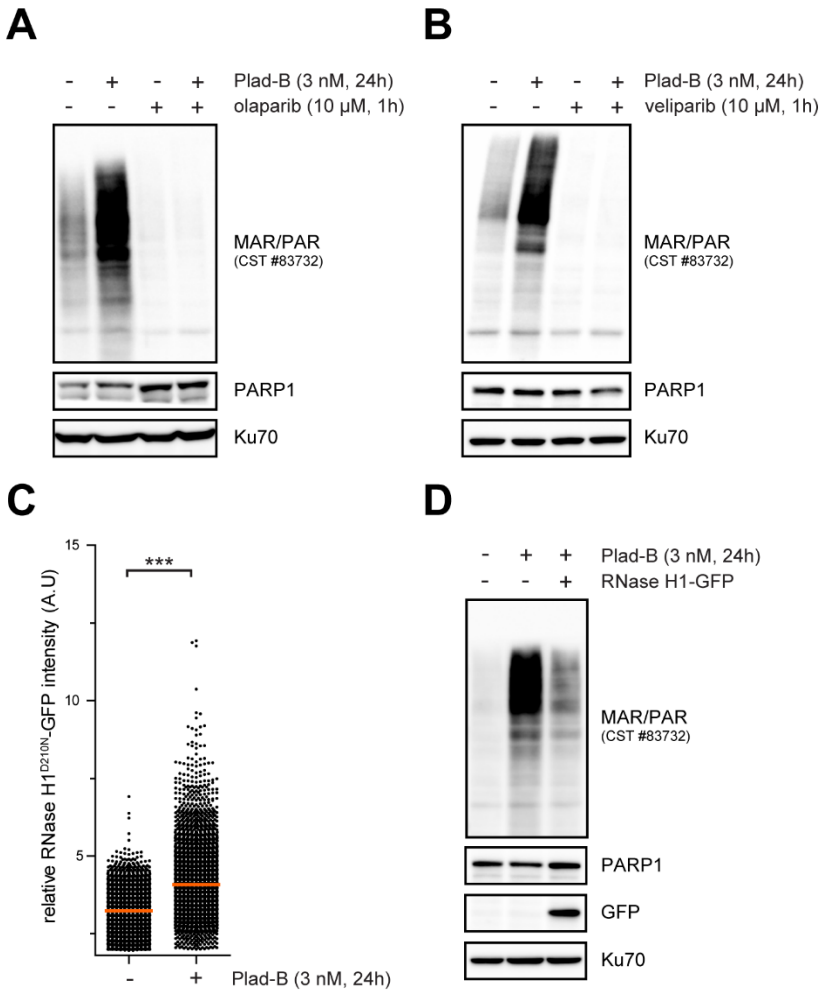

Figure 1. RNA splicing perturbation by Plad-B elicits PARP response through R-loops. (A) HeLa cells were treated with DMSO (-), or pladienolide-B (Plad-B; 3 nM and 24h) in the presence or absence of olaparib (10 μM and 1h) or **(B)** veliparib (10 μM and 1h) followed by assessment of MAR/PAR and PARP1 levels by immunoblot. **(C)** HeLa cells inducibly expressing nuclear RNase $H1^{D210N}$-GFP were treated with DMSO or Plad-B (3 nM and 24h) followed by immunofluorescence. GFP intensity of individual cells were analyzed (n>3600). Red bars represent the mean γH2AX level in the indicated groups. Statistical analysis was performed using unpaired two-tailed Student's t-test (***, p<0.001). **(D)** HeLa cells that inducibly express nuclear RNase H1-GFP were treated with either DMSO or Plad-B (3 nM and 24h), followed by MAR/PAR levels assessment by immunoblot.

RNA splicing perturbation by Plad-B induces ADP-ribosylation is mediated by both PARP1 and PARP2.

Since PARP inhibitors, olaparib and veliparib, target both PARP1/2 enzymes[47], we next asked which enzymes are important for PARP activation. First, we singly deleted *PARP1* or *PARP2* gene by CRISPR-Cas9 to generate PARP1^{KO} and PARP2^{KO} HeLa cells, respectively. To functionally validate our knockout cell lines, we treated wildtype and PARP1^{KO} and PARP2^{KO} HeLa cells with hydrogen peroxide (H_2O_2), a commonly used chemical to trigger ADP-ribosylation caused by high reactive oxidative stress. Consistent with previous reports[40,48,49], we validated that PARP1^{KO}, but not PARP2^{KO}, HeLa cells completely abrogated H_2O_2-induced MAR/PAR levels using two different antibodies, MAR/PAR and anti-pan-ADP-ribose binding reagent, pan-ADPr (Figures 2A). These data suggest that PARP1 plays a major role in H_2O_2-induced DNA damage response.

Next, we asked whether PARP1 also plays a role in Plad-B-induced ADP-ribosylation. We treated wildtype and PARP1^{KO} cells with Plad-B for 24 hours and monitored PARP activity in total cell extracts. Deletion of *PARP1* completely abrogated elevated MAR/PAR levels, suggesting that Plad-B-induced ADP-ribosylation is PARP1 dependent (Figure 2B). To address whether PARP1 enzymatic activity is essential for ADP-ribosylation, we overexpressed either Flag-tagged PARP1^{WT}, PARP1^{7KQ}, or PARP1^{E988K} mutants in PARP1^{KO} cells. PARP1^{7KQ} mutant disrupts serine ADP-ribosylation and greatly inhibits auto-modification of PARP1, thereby reducing PARP1 activity[50]. PARP1^{E988K}, a PARylation-deficient PARP1, loses its PARylation activity but retains some MARylation activity[51]. Overexpression of Flag-tagged PARP1^{WT}, but not PARP1^{7KQ} mutant, rescued Plad-B induced MAR/PAR levels in PARP1^{KO} HeLa cells (Figure 2C). Similarly, PARP1^{E988K}, but not PARP1^{WT}, also failed to rescue Plad-B-induced MAR/PAR levels in PARP1^{KO} cells (Figure 2D). These results suggest that PARP1 activity is required for Plad-B induced ADP-ribosylation. Surprisingly, PARP2^{KO} cells also reduced Plad-B-induced MAR/PAR levels, but not completely

abrogated as observed in PARP1^{KO} cells (Figure 2E). Similar reduced MAR/PAR levels were observed in a second PARP2^{KO} cell line, generated using an independent gRNA sequence (PARP2$^{KO\ \#2}$). In addition, the reduced MAR/PAR levels in PARP2^{KO} cells were also observed using the pan-ADPr antibody (Figure 2F). Taken together, these results suggest that RNA splicing perturbation by Plad-B induces R-loops and elicits a unique PARP response mediated by both PARP1 and PARP2, which is in stark contrast to the PARP1-dependent, but PARP2-independent functions in H_2O_2-induced DNA damage context.

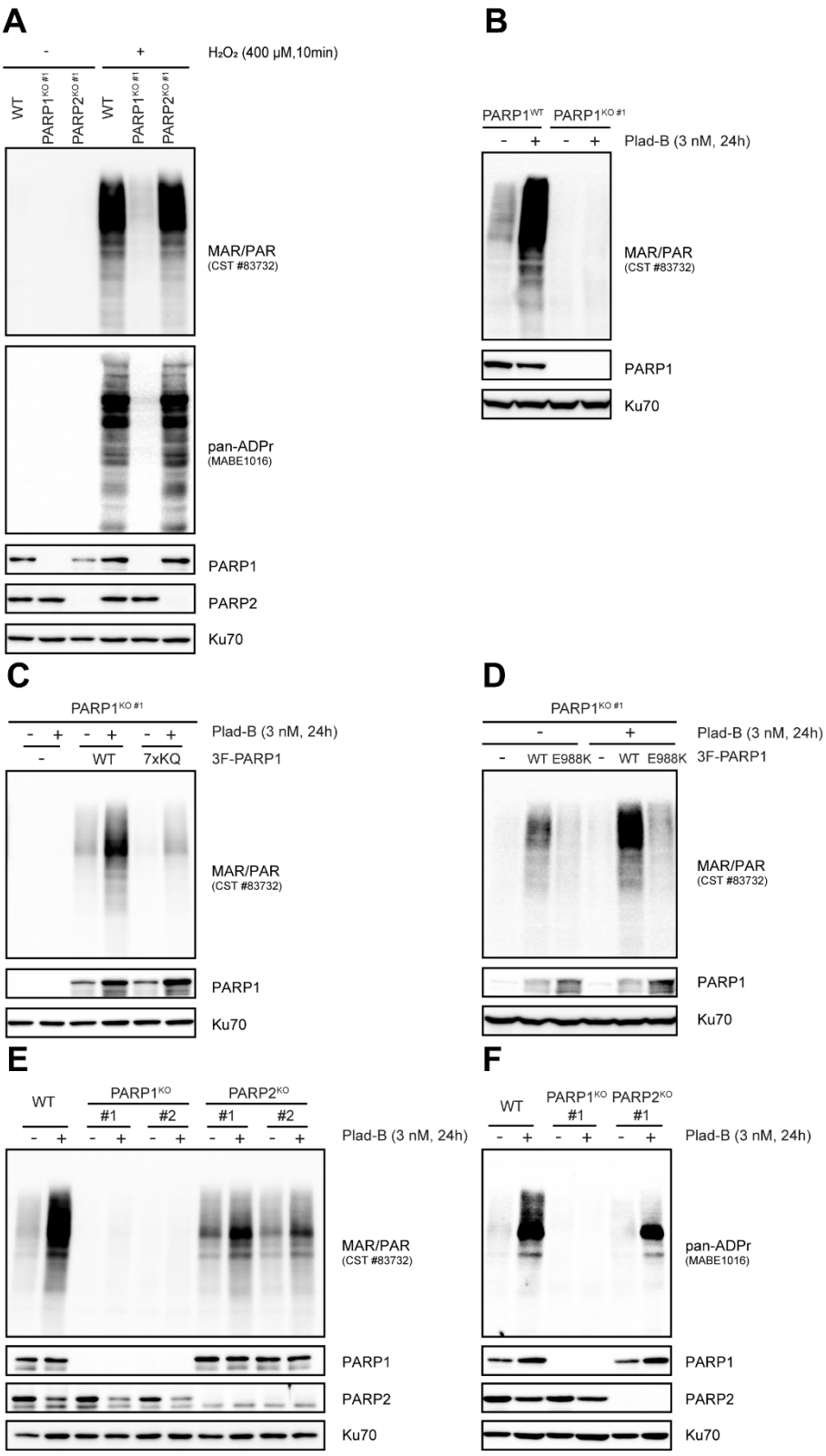
A
-
+
H₂O₂ (400 μM,10min)
WT
PARP1KO #1
PARP2KO #1
WT
PARP1KO #1
PARP2KO #1
MAR/PAR
(CST #83732)
pan-ADPr
(MABE1016)
PARP1
PARP2
Ku70
B
PARP1WT
PARP1KO #1
- + - +
Plad-B (3 nM, 24h)
MAR/PAR
(CST #83732)
PARP1
Ku70
C
PARP1KO #1
- + - + - +
Plad-B (3 nM, 24h)
- WT 7xKQ
3F-PARP1
MAR/PAR
(CST #83732)
PARP1
Ku70
D
PARP1KO #1
- +
Plad-B (3 nM, 24h)
- WT E988K - WT E988K
3F-PARP1
MAR/PAR
(CST #83732)
PARP1
Ku70
E
WT
PARP1KO
#1 #2
PARP2KO
#1 #2
- + - + - + - + - +
Plad-B (3 nM, 24h)
MAR/PAR
(CST #83732)
PARP1
PARP2
Ku70
F
WT
PARP1KO
#1
PARP2KO
#1
- + - + - +
Plad-B (3 nM, 24h)
pan-ADPr
(MABE1016)
PARP1
PARP2
Ku70

Figure 2. PARP1 and PARP2 enzymes play important roles in the PARP activity in Plad-B-treated cells. (A) Parental, *PARP1*-knockout or *PARP2*-knockout HeLa cells were treated with Hydrogen peroxide (H_2O_2; 400 µM and 10min) followed by assessment of PARP1, PARP2, MAR/PAR, and pan-ADPr levels by immunoblot. **(B)** Parental or *PARP1*-knockout HeLa cells were treated with Plad-B (24h and 3 nM) followed by assessment of MAR/PAR and PARP1 levels by immunoblot. **(C)** *PARP1*-knockout HeLa cells overexpressing either wild-type (WT), an inactive form (7KQ) of PARP1, or **(D)** another inactive form (E988K) of PARP1 cDNA were treated with Plad-B (24h and 3 nM) followed by assessment of total PARylation. **(E)** Parental, *PARP1*-knockout or *PARP2*-knockout HeLa cells were treated with Plad-B (24h and 3 nM). PARP activity was measured using MAR/PAR mAb, and **(F)** pan-ADPr binding reagent by immunoblot.

RNA splicing perturbation by Plad-B elicits PARP1/2 response to prevent DNA damage.

To evaluate the functional consequences of PARPi on Plad-B treated cells, we monitored levels of both MAR/PAR and γH2AX, a marker of DNA damage, in cells treated with Plad-B for 24h in the presence or absence olaparib. In the absence of olaparib, Plad-B treated cells exhibited higher MAR/PAR levels than wildtype cells (Figure 3A). Co-treatment of Plad-B and olaparib for 24h completely abrogated Plad-B-induced MAR/PAR levels that coincide with an induction of γH2AX levels (Figure 3A). Moreover, the γH2AX levels was significantly higher in combined Plad-B and olaparib than individual drug treatment alone or DMSO-treated as observed by immunofluorescence (Figure 3B and C). Taken together, these results suggest that RNA splicing perturbation by Plad-B treatment creates a reliance on PARP1/2 activity to prevent DNA damage.

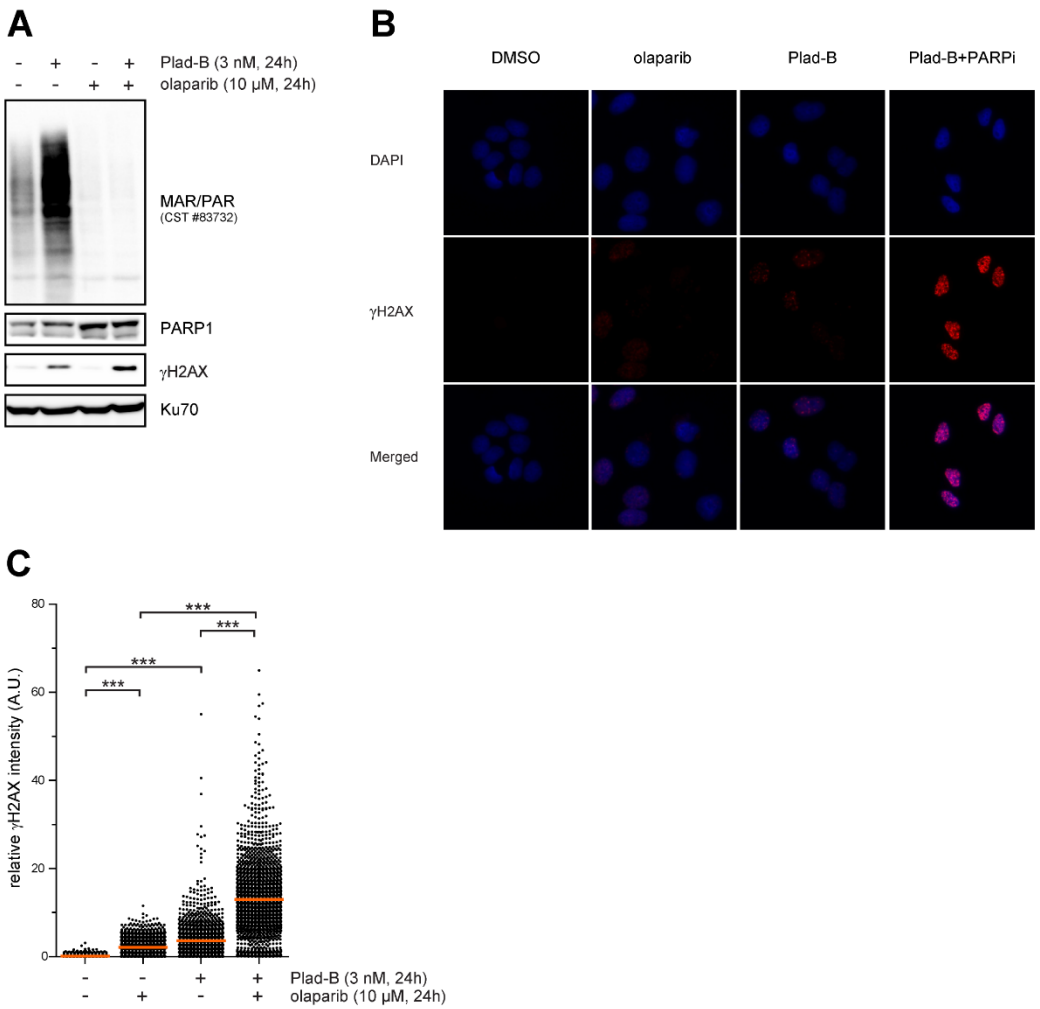

Figure 3. Plad-B treated cells required PARP1/2 activity to prevent DNA damage. (A) HeLa cells treated with DMSO (-), olaparib (10 μM and 24h), Plad-B (24h and 3 nM), or combined PARPi+Plad-B followed by assessment of PAR and γH2AX levels by immunoblot, or by **(B-C)** immunofluorescence, where γH2AX intensity of individual cells were analyzed (n>3600). Red bars represent the mean γH2AX level in the indicated groups Statistical analysis was performed using unpaired two-tailed Student's t-test (***, $p<0.001$).

RNA splicing perturbation by MS023 elicits PARP1/2 response arises from R-loop accumulation.

The surprising link between RNA splicing perturbation by Plad-B, R-loop, and PARP1/2 response led us to ask whether the same phenomenon would be observed using other pharmacologic splicing modulators. To address this question, we used MS023, a compound that inhibits Type I protein arginine methyltransferases (PRMTs) by suppressing symmetric or asymmetric dimethylation of arginine[46]. Treatment of MS023 was previously shown to reduce splicing fidelity and to promote alternative splicing[44]. We treated cells with MS023 in HeLa cells to monitor PARP response. Similar to Plad-B treatment, MS023 elicited an increased ADP-ribosylation (Figure 4A). PARP1^{KO} cells completely abrogated MS023-induced MAR/PAR levels. Importantly, PARP2^{KO} cells also reduced elevated MAR/PAR levels (Figure 4A). Similar reduction in MAR/PAR levels was observed using a second antibody, pan-ADPr (Figure 4A, lower panel). Moreover, 24h PARPi treatment completely suppressed increased level of PAR by 24h MS023 treatment (Figure 4B). To test whether PARP response induced by MS023 arises from R-loops, we treated RNase H1-GFP HeLa cells with MS023 in the presence or absence of doxycycline to induce RNase H1 expression. Induction of RNase H1 in MS023 treated cells reduced MAR/PAR levels, showing that MS023 induced increase in MAR/PAR levels is R-loop dependent (Figure 4C). Taken together, these data demonstrate that both PARP1 and PARP2 enzymes are critical to elicit a robust ADP-ribosylation response in MS023-treated cells that arise from accumulated R-loops.

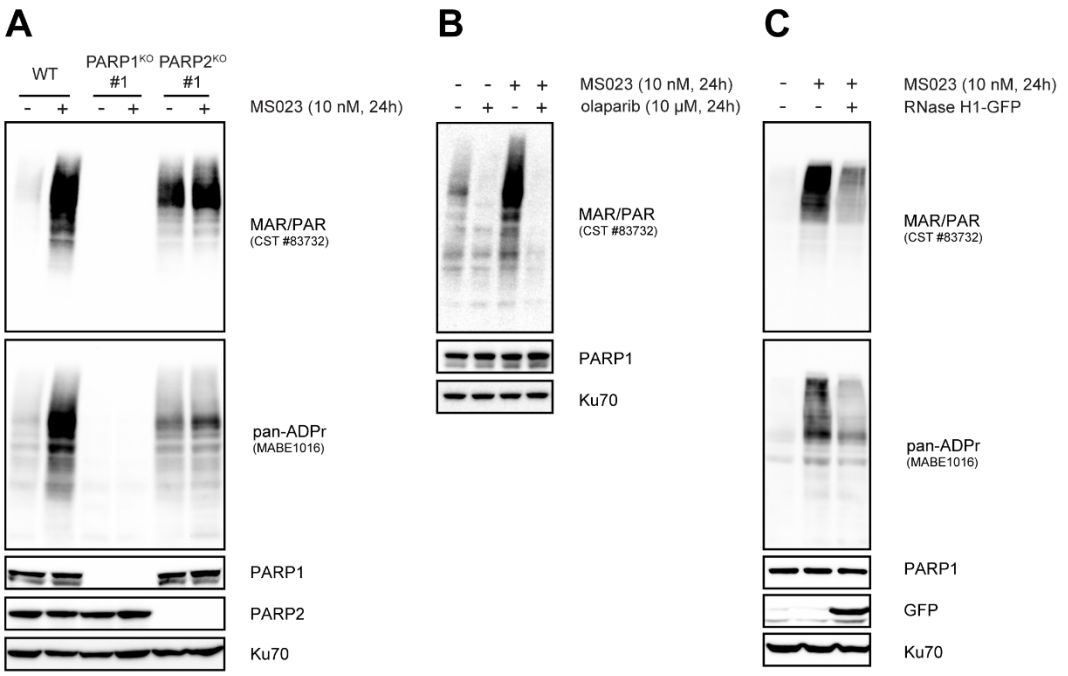

Figure 4. MS023 induced perturbation in RNA splicing elicits PARP response through R-loops. (A) Parental, *PARP1*-knockout or *PARP2*-knockout HeLa cells were treated with MS023 (10 nM, 24h) followed by assessment of MAR/PAR and pan-ADPr levels by immunoblot. **(B)** HeLa cells were treated with DMSO (-), or MS023 (10 nM, 24h) in the presence or absence of olaparib (PARPi) (10 μM and 1h) followed by assessment of MAR/PAR levels by immunoblot. **(C)** HeLa cells inducibly expressing nuclear RNase H1 were treated with Plad-B (3 nM, 24h) or DMSO followed by MAR/PAR and pan-ADPr levels assessment by immunoblot.

PARP1 BRCT domain and activity is required for replication protein A (RPA) interaction.

The link between R-loop accumulation and PARP1 response led us to wonder how PARP1 enzyme is recruited to R-loops. We previously identified that RPA-coated ssDNA is a potential sensor of R Loops. Thus, we investigated whether PARP1 recruitment to R-loop could be mediated through RPA interaction. We overexpressed flag-tagged wildtype PARP1 in HeLa cells and immunoprecipitated using anti-Flag antibody. Immunoprecipitation of Flag-tagged wild-type PARP1 captured endogenous RPA7, a subunit of RPA complex (Figure 5A). This result suggests that RPA-ssDNA at R-loops could facilitate PARP1 recruitment and activity.

PARP1 comprises of three main domains including an N-terminal DNA-binding domain (residues 1–353), an auto-modification domain (residues 389–643), and a catalytic domain in the C-terminal (CAT) (residues 662–1014). Three zinc finger domains are DNA-binding domains. ZnFI and ZnFII are required for recognition and binding to DNA damage sites, while ZnFIII has an important role in the enzyme activation upon DNA binding. The central auto-modification domain composed of a breast cancer type 1 susceptibility protein (BRCA1), C-terminal (BRCT) motif, and the WGR domain serves as the sites for PARylation. BRCT motif mediates protein–protein interactions, while the WGR domain interacts with ZnFI, ZnFIII, CAT, and the DNA and is important for DNA-dependent activity of the catalytic domain[51]. To determine PARP1 domains that promotes RPA interaction, we generated a point PARP1 mutation ($PARP1^{E988K}$) and truncation mutants without the BRCT domain ($PARP1^{\Delta BRCT}$), the WGR domain ($PARP1^{\Delta WGR}$), or all of the domains except for the ZnF domains ($PARP1^{ZnF}$) (Figure 5B). To evaluate the interaction efficiency across different mutants, we measured the ratio of immunoprecipitated RPA70 normalized to the amount of Flag-tagged PARP1 pulldown. Similar to wild-type PARP1, $PARP1^{\Delta WGR}$ did not affect its RPA interaction (Figure 5C). Interestingly, $PARP1^{ZnF}$ and $PARP1^{\Delta BRCT}$ decreased the RPA interaction. $PARP1^{E988K}$ dramatically reduced the interaction with

RPA (Figure 5C). Taken together, these data suggest that RPA interaction is mediated through PARP1's BRCT domain and is required PARP1 enzymatic activity.

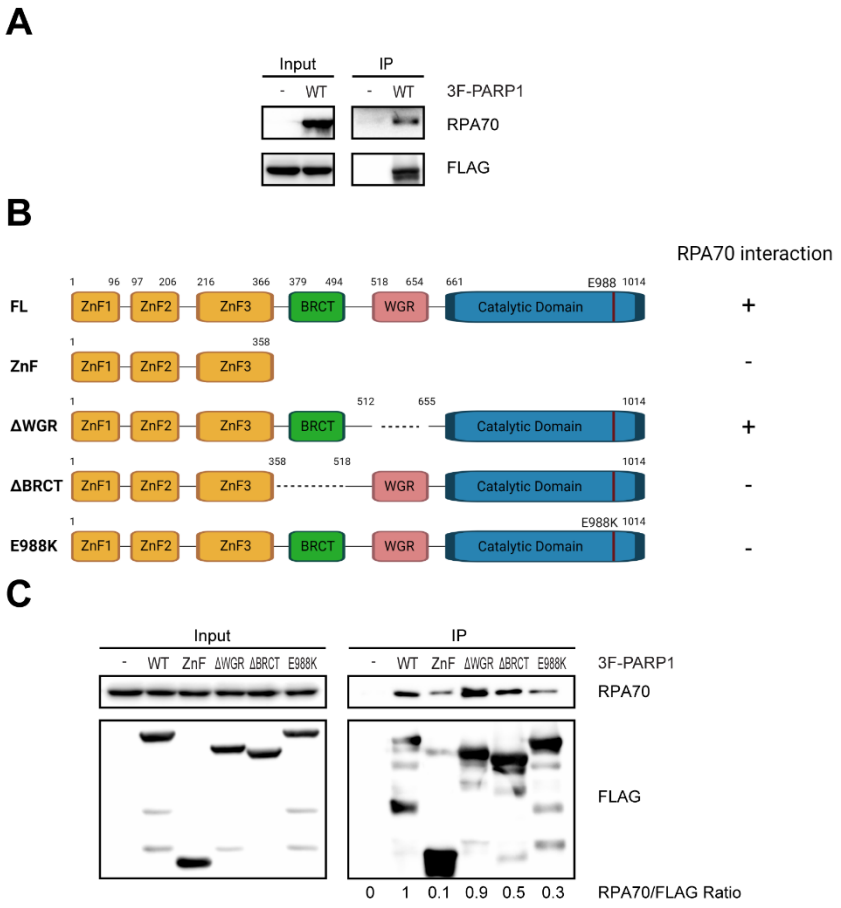

Figure 5. PARP1 potentially interact with replication protein A (RPA) to suppress R-loops in cancer cells. (A) Diagrams (not to scale) of full length, point mutation, and truncated human PARP1. ZnFI: zinc finger I, ZnFII: zinc finger II, ZnFIII: zinc finger III, BRCT: BRCA1 C-terminal. The major domains and active catalytic sites are marked. **(B)** HeLa cells were transfected with *PARP1*^{WT}, **(C)** *PARP*^{ZnF}, *PARP1*$^{\Delta WGR}$, *PARP1*$^{\Delta BRCT}$, and *PARP1*^{E988K}. Level of RPA70 and Flag were analyzed by PARP1 immunoprecipitation and western blot.

Discussion

Here, we identified that RNA splicing modulators, Plad-B and MS023 elicited a poly ADP-ribosylation response in an R-loop dependent manner. PARP inhibitor, olaparib, induced more DNA damage in cells treated Plad-B, suggesting a new synthetic lethality modality. Surprisingly, both PARP1 and PARP2 enzymes are important for the PARP response in Plad-B- and MS023-treated cells, which is in contrast to their known functions where PARP1 plays the major role in DNA repair. Importantly, our results also highlight a potential of combining RNA splicing modulators and PARP inhibitors to treat MDS patients harboring splicing factor mutations.

PARP1 is a member of Poly (ADP-Ribose) Polymerases (PARPs) family which catalyze Poly ADP-ribosylation (PARylation) chain to itself and to multiple target proteins during DNA repair, stabilization of replication forks, modification of chromatin structures, and transcriptional regulation[38,40]. In the previous research, we identified that PARP functions are required to promote splicing factor mutant cell survival, preventing accumulated DNA damage arising from aberrant R-loop accumulation. Splicing factor mutant cells are sensitive to PARPi, highlighting that PARPi could be a potential therapeutic agent for MDS or other cancers harboring splicing factor mutations. Here, we demonstrated that RNA splicing perturbation by splicing modulators, such as Plad-B and MS023, promoting the aberrant accumulation of R-loop activates PARP response for survival in HeLa cells. These data provide potential rationale to combine PARPi with RNA splicing modulators that improve therapeutic efficacy for MDS patients harboring splicing factor mutations. Future study will be important to test the combination of RNA splicing modulators and PARP inhibitors sensitize splicing factor mutant MDS/sAML in clinical models. One splicing modulator has entered clinical trials. H3B-8800 is orally bioavailable and appears efficacious against tumors with splicing factor mutations, not limited to SF3B1 but also encompassing U2AF1 and SRSF2[52]. Additionally, four PARP inhibitors have been approved by FDA in various indications: olaparib, niraparib, and rucaparib in high-

grade serous ovarian cancers, and olaparib and talazoparib in metastatic breast cancers[53]. Therefore, which combination of splicing modulator and PARPi is much more efficient in MDS or other myeloid malignancies that harbor different splicing factor mutations warrants further investigation.

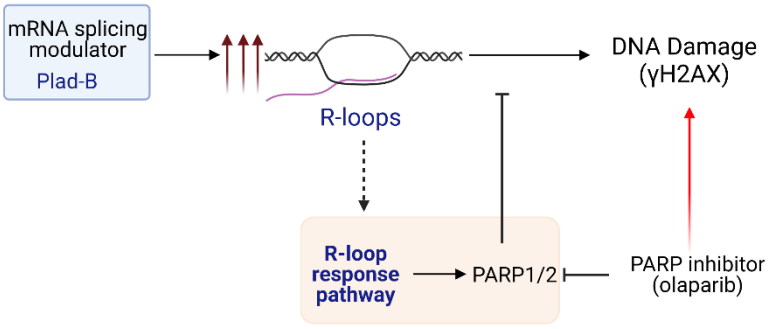

Figure 6. Summary. The panel shows that mRNA splicing modulator trigger the aberrant accumulation of R-loops to render cells more dependent on PARP1 activity to prevent R-loop-associated genomic instability. Therefore, combining Plad-B with PARPi induced higher DNA damage in an R-loop-dependent manner.

Previously, we identified RPA is a key sensor of R-loops and binds to the displaced ssDNA at R-loops[26]. The RPA-coated ssDNA at R-loops may recruit and associate with PARP1 through the interaction between RPA and PARP1. In line with this notion, we identified that RPA interacts with PARP1 mediated through BRCT domain (Figure 5). Interestingly, PARP1 activity is also required. It will be important to determine whether PARP1 activity promotes PARP1 recruitment to R-loops or stabilizing PARP1 association to R-loops. Alternatively, RPA-PARP1 interaction may be in complex with other R-loop regulators, such as DXH9, or XRN2 [54,55]. Future studies will be necessary to pinpoint how PARP1 recognizes R-loops and how PARP1 activity regulates R-loops to prevent DNA damage.

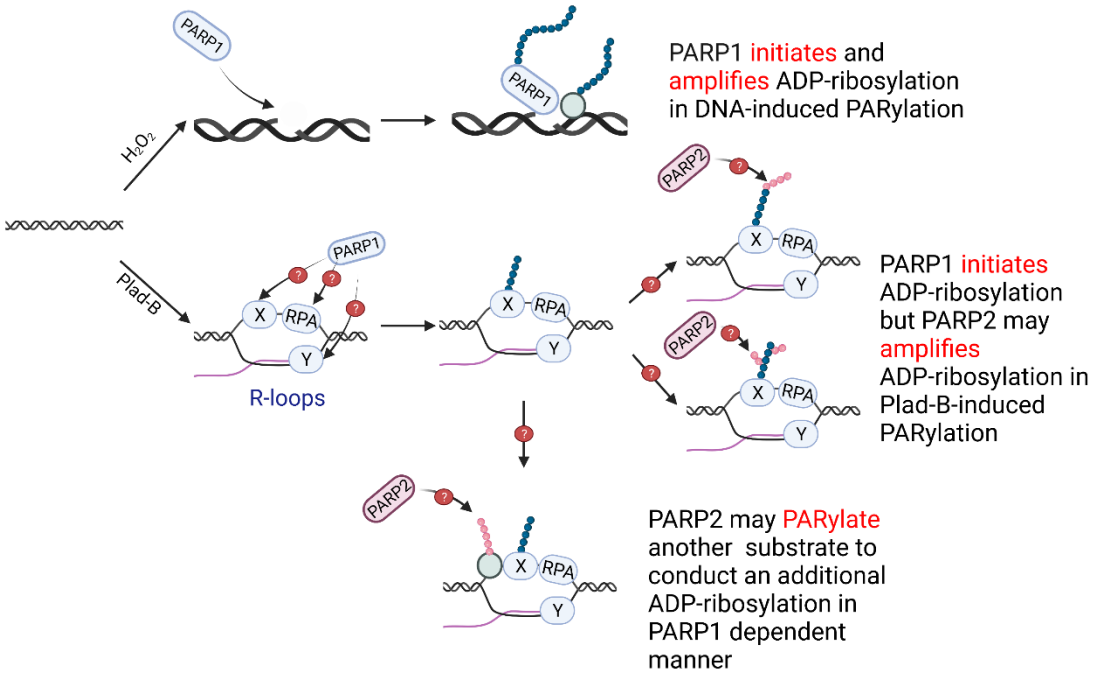

Figure 7. Proposal model for PARP1/2 functions in R-loop regulation. A proposal model shows two modes of PARP1/2 response. In H_2O_2 treatment, PARP1 is recruited to DNA damage site. PARP1, but not PARP2, initiates and amplifies the major ADP-ribosylation. In Plad-B treatment, PARP1 is associated with R-loops and initiates ADP-ribosylation. PARP2 may amplify the rest of ADP-ribosylation through conducting either linear or branched PARylation, or conduct new PAR chain by modifying another substrate in PARP1 dependent manner.

In this study, we surprisingly found that both PARP1 and PARP2 are required to mount robust ADP-ribosylation response to RNA splicing modulators. This is in contrast to H_2O_2-induced PARylation where only PARP1, but not PARP2, is required. Here, we propose a two-step model where PARP1 first primes ADP-ribosylation at R-loops and PARP2 then amplifies ADP-ribosylation. How PARP2 amplifies ADP-ribosylation at R-loops is not known. It possible that PARP2 extends existing the ADP-ribosylated chains catalyzed PARP1. Alternatively, PARP2 may be recruited by the MAR/PAR chains primed by PARP1 and subsequently ADP-ribosylates additional proteins.

Finally, PARP2 may catalyze either linear and branched PAR chains as recently reported[56]. Future studies are needed to better understand how PARP1 and PARP2 regulates R-loops. Importantly, these mechanistic insights may provide additional PARP1 and/or PARP2 substrates as potential therapeutic biomarkers for PARPi sensitivity or new targets for future targeted therapeutic development.

The increased DNA damage caused be the combined splicing modulator and PARPi highlight a potential new drug combination to treat MDS patients harboring splicing factor mutations. Additionally, The Cancer Genome Atlas (TCGA) highlighted that 119 splicing factor genes carry putative driver mutations over 33 tumor types[57] such as chronic lymphocytic leukemia (CLL), clonal hematopoiesis (CH), mantle cell lymphoma (MCL)[58], and solid tumors including adenoid cystic carcinoma, breast cancer, pancreatic cancer, bladder carcinoma, skin cutaneous melanoma, and lung adenocarcinoma[57,59–63]. Therefore, future studies will also be important to test which cancer mutations induce aberrant accumulation of R-loops. If aberrant R-loop accumulation is a common cellular response in these cancers, targeting PARP1/2 response pathway could also be a potentially targeted therapy for cancers beyond myeloid malignancies. Importantly, our results highlight that FDA-approved PARP inhibitors could be potentially therapeutic agents to treat myeloid malignancies or other cancers harboring splicing factor mutations either as a monotherapy or in combination with RNA splicing modulators.

Bibliography

1. Ma, X. Epidemiology of myelodysplastic syndromes. *Am J Med* **125**, S2-5 (2012).
2. Raza, A. & Galili, N. The genetic basis of phenotypic heterogeneity in myelodysplastic syndromes. *Nat Rev Cancer* **12**, 849–859 (2012).
3. Schwind, S., Jentzsch, M., Kubasch, A. S., Metzeler, K. H. & Platzbecker, U. Myelodysplastic syndromes: Biological and therapeutic consequences of the evolving molecular aberrations landscape. *Neoplasia* **23**, 1101–1109 (2021).
4. Scott, B. L. & Deeg, H. J. Myelodysplastic syndromes. *Annu Rev Med* **61**, 345–358 (2010).
5. Goldberg, S. L. *et al.* Incidence and clinical complications of myelodysplastic syndromes among United States Medicare beneficiaries. *J Clin Oncol* **28**, 2847–2852 (2010).
6. Greenberg, P. *et al.* International scoring system for evaluating prognosis in myelodysplastic syndromes. *Blood* **89**, 2079–2088 (1997).
7. Troy, J. D., Atallah, E., Geyer, J. T. & Saber, W. Myelodysplastic syndromes in the United States: an update for clinicians. *Ann Med* **46**, 283–289 (2014).
8. Platzbecker, U., Kubasch, A. S., Homer-Bouthiette, C. & Prebet, T. Current challenges and unmet medical needs in myelodysplastic syndromes. *Leukemia* **35**, 2182–2198 (2021).
9. Germing, U. *et al.* Novel therapies in low- and high-risk myelodysplastic syndrome. *Expert Rev Hematol* **12**, 893–908 (2019).
10. Gil-Perez, A. & Montalban-Bravo, G. Management of myelodysplastic syndromes after failure of response to hypomethylating agents. *Ther Adv Hematol* **10**, 2040620719847059 (2019).
11. de Witte, T. *et al.* Allogeneic hematopoietic stem cell transplantation for MDS and CMML: recommendations from an international expert panel. *Blood* **129**, 1753–1762 (2017).
12. Lindholm, C. *et al.* Failure to reach hematopoietic allogenic stem cell transplantation in patients with myelodysplastic syndromes planned for transplantation: a population-based study. *Bone Marrow Transplant* **57**, 598–606 (2022).
13. Festuccia, M. *et al.* Hematopoietic Cell Transplantation in Myelodysplastic Syndromes after Treatment with Hypomethylating Agents. *Biol Blood Marrow Transplant* **23**, 1509–1514 (2017).
14. Thol, F. *et al.* Frequency and prognostic impact of mutations in SRSF2, U2AF1, and ZRSR2 in patients with myelodysplastic syndromes. *Blood* **119**, 3578–3584 (2012).

15. Visconte, V. *et al.* SF3B1, a splicing factor is frequently mutated in refractory anemia with ring sideroblasts. *Leukemia* **26**, 542–545 (2012).
16. Papaemmanuil, E. *et al.* Clinical and biological implications of driver mutations in myelodysplastic syndromes. *Blood* **122**, 3616–3627; quiz 3699 (2013).
17. Saez, B., Walter, M. J. & Graubert, T. A. Splicing factor gene mutations in hematologic malignancies. *Blood* **129**, 1260–1269 (2017).
18. Yip, B. H. *et al.* The U2AF1S34F mutation induces lineage-specific splicing alterations in myelodysplastic syndromes. *J Clin Invest* **127**, 2206–2221 (2017).
19. Komeno, Y. *et al.* SRSF2 Is Essential for Hematopoiesis, and Its Myelodysplastic Syndrome-Related Mutations Dysregulate Alternative Pre-mRNA Splicing. *Mol Cell Biol* **35**, 3071–3082 (2015).
20. Alsafadi, S. *et al.* Cancer-associated SF3B1 mutations affect alternative splicing by promoting alternative branchpoint usage. *Nat Commun* **7**, 10615 (2016).
21. Lamond, A. I. The spliceosome. *Bioessays* **15**, 595–603 (1993).
22. Konarska, M. M., Grabowski, P. J., Padgett, R. A. & Sharp, P. A. Characterization of the branch site in lariat RNAs produced by splicing of mRNA precursors. *Nature* **313**, 552–557 (1985).
23. Will, C. L. & Lührmann, R. Spliceosome structure and function. *Cold Spring Harb Perspect Biol* **3**, a003707 (2011).
24. Dvinge, H. & Bradley, R. K. Widespread intron retention diversifies most cancer transcriptomes. *Genome Med* **7**, 45 (2015).
25. Joshi, P., Halene, S. & Abdel-Wahab, O. How do messenger RNA splicing alterations drive myelodysplasia? *Blood* **129**, 2465–2470 (2017).
26. Nguyen, H. D. *et al.* Functions of Replication Protein A as a Sensor of R Loops and a Regulator of RNaseH1. *Mol Cell* **65**, 832-847.e4 (2017).
27. Matos, D. A. *et al.* ATR Protects the Genome against R Loops through a MUS81-Triggered Feedback Loop. *Molecular Cell* **77**, 514-527.e4 (2020).
28. Yu, K., Chedin, F., Hsieh, C.-L., Wilson, T. E. & Lieber, M. R. R-loops at immunoglobulin class switch regions in the chromosomes of stimulated B cells. *Nat Immunol* **4**, 442–451 (2003).
29. Ginno, P. A., Lott, P. L., Christensen, H. C., Korf, I. & Chédin, F. R-loop formation is a distinctive characteristic of unmethylated human CpG island promoters. *Mol Cell* **45**, 814–825 (2012).
30. Skourti-Stathaki, K., Kamieniarz-Gdula, K. & Proudfoot, N. J. R-loops induce repressive chromatin marks over mammalian gene terminators. *Nature* **516**, 436–439 (2014).
31. Gan, W. *et al.* R-loop-mediated genomic instability is caused by impairment of

replication fork progression. *Genes Dev* **25**, 2041–2056 (2011).
32. Li, M., Pokharel, S., Wang, J.-T., Xu, X. & Liu, Y. RECQ5-dependent SUMOylation of DNA topoisomerase I prevents transcription-associated genome instability. *Nat Commun* **6**, 6720 (2015).
33. Cohen, S. *et al.* Senataxin resolves RNA:DNA hybrids forming at DNA double-strand breaks to prevent translocations. *Nat Commun* **9**, 533 (2018).
34. De, I. *et al.* The RNA helicase Aquarius exhibits structural adaptations mediating its recruitment to spliceosomes. *Nat Struct Mol Biol* **22**, 138–144 (2015).
35. Maréchal, A. & Zou, L. RPA-coated single-stranded DNA as a platform for post-translational modifications in the DNA damage response. *Cell Res* **25**, 9–23 (2015).
36. Paulsen, R. D. *et al.* A Genome-wide siRNA Screen Reveals Diverse Cellular Processes and Pathways that Mediate Genome Stability. *Molecular Cell* **35**, 228–239 (2009).
37. Nguyen, H. D. *et al.* Spliceosome Mutations Induce R Loop-Associated Sensitivity to ATR Inhibition in Myelodysplastic Syndromes. *Cancer Res* **78**, 5363–5374 (2018).
38. Alemasova, E. E. & Lavrik, O. I. Poly(ADP-ribosyl)ation by PARP1: reaction mechanism and regulatory proteins. *Nucleic Acids Res* **47**, 3811–3827 (2019).
39. Vyas, S., Chesarone-Cataldo, M., Todorova, T., Huang, Y.-H. & Chang, P. A systematic analysis of the PARP protein family identifies new functions critical for cell physiology. *Nat Commun* **4**, 2240 (2013).
40. Beck, C., Robert, I., Reina-San-Martin, B., Schreiber, V. & Dantzer, F. Poly(ADP-ribose) polymerases in double-strand break repair: focus on PARP1, PARP2 and PARP3. *Exp Cell Res* **329**, 18–25 (2014).
41. Yokoi, A. *et al.* Biological validation that SF3b is a target of the antitumor macrolide pladienolide. *FEBS J* **278**, 4870–4880 (2011).
42. Kotake, Y. *et al.* Splicing factor SF3b as a target of the antitumor natural product pladienolide. *Nat Chem Biol* **3**, 570–575 (2007).
43. Lagisetti, C. *et al.* Synthetic mRNA splicing modulator compounds with in vivo antitumor activity. *J Med Chem* **52**, 6979–6990 (2009).
44. Fong, J. Y. *et al.* Therapeutic Targeting of RNA Splicing Catalysis through Inhibition of Protein Arginine Methylation. *Cancer Cell* **36**, 194-209.e9 (2019).
45. Koh, C. M. *et al.* MYC regulates the core pre-mRNA splicing machinery as an essential step in lymphomagenesis. *Nature* **523**, 96–100 (2015).
46. Eram, M. S. *et al.* A Potent, Selective, and Cell-Active Inhibitor of Human Type I Protein Arginine Methyltransferases. *ACS Chem Biol* **11**, 772–781 (2016).
47. Murai, J. *et al.* Trapping of PARP1 and PARP2 by Clinical PARP Inhibitors. *Cancer Res* **72**, 5588–5599 (2012).

48. Kutuzov, M. M., Belousova, E. A., Ilina, E. S. & Lavrik, O. I. Impact of PARP1, PARP2 & PARP3 on the Base Excision Repair of Nucleosomal DNA. *Adv Exp Med Biol* **1241**, 47–57 (2020).
49. Ghosh, R., Roy, S., Kamyab, J., Danzter, F. & Franco, S. Common and unique genetic interactions of the poly(ADP-ribose) polymerases PARP1 and PARP2 with DNA double-strand break repair pathways. *DNA Repair (Amst)* **45**, 56–62 (2016).
50. Liszczak, G., Diehl, K. L., Dann, G. P. & Muir, T. W. Acetylation blocks DNA damage-induced chromatin ADP-ribosylation. *Nat Chem Biol* **14**, 837–840 (2018).
51. Shao, Z. *et al.* Clinical PARP inhibitors do not abrogate PARP1 exchange at DNA damage sites in vivo. *Nucleic Acids Research* **48**, 9694–9709 (2020).
52. Seiler, M. *et al.* H3B-8800, an orally available small-molecule splicing modulator, induces lethality in spliceosome-mutant cancers. *Nat Med* **24**, 497–504 (2018).
53. Redelico, T. Rucaparib and Niraparib in Advanced Ovarian Cancer. *J Adv Pract Oncol* **10**, 402–408 (2019).
54. Cristini, A., Groh, M., Kristiansen, M. S. & Gromak, N. RNA/DNA Hybrid Interactome Identifies DXH9 as a Molecular Player in Transcriptional Termination and R-Loop-Associated DNA Damage. *Cell Rep* **23**, 1891–1905 (2018).
55. Patidar, P. L. *et al.* XRN2 interactome reveals its synthetic lethal relationship with PARP1 inhibition. *Sci Rep* **10**, 14253 (2020).
56. Chen, Q., Kassab, M. A., Dantzer, F. & Yu, X. PARP2 mediates branched poly ADP-ribosylation in response to DNA damage. *Nat Commun* **9**, 3233 (2018).
57. Seiler, M. *et al.* Somatic Mutational Landscape of Splicing Factor Genes and Their Functional Consequences across 33 Cancer Types. *Cell Rep* **23**, 282-296.e4 (2018).
58. Chen, S., Benbarche, S. & Abdel-Wahab, O. Splicing factor mutations in hematologic malignancies. *Blood* **138**, 599–612 (2021).
59. Martelotto, L. G. *et al.* Genomic landscape of adenoid cystic carcinoma of the breast. *J Pathol* **237**, 179–189 (2015).
60. Cancer Genome Atlas Network. Comprehensive molecular portraits of human breast tumours. *Nature* **490**, 61–70 (2012).
61. Biankin, A. V. *et al.* Pancreatic cancer genomes reveal aberrations in axon guidance pathway genes. *Nature* **491**, 399–405 (2012).
62. Martin, M. *et al.* Exome sequencing identifies recurrent somatic mutations in EIF1AX and SF3B1 in uveal melanoma with disomy 3. *Nat Genet* **45**, 933–936 (2013).
63. Brooks, A. N. *et al.* A pan-cancer analysis of transcriptome changes associated with somatic mutations in U2AF1 reveals commonly altered splicing events. *PLoS One* **9**, e87361 (2014).